J. Synchrotron Rad. (1998). **5**, 506–508

First performance assessment of the small-angle X-ray scattering beamline at ELETTRA

H. Amenitsch,[a]* M. Rappolt,[a] M. Kriechbaum,[a] H. Mio,[a] P. Laggner[a] and S. Bernstorff[b]

[a]Institute of Biophysics and X-ray Structure Research, Austrian Academy of Sciences, Steyrergasse 17, A-8010 Graz, Austria, and [b]Sincrotrone Trieste, Experimental Division, SS 14, Km 163.5, I-34012 Basovizza, (TS), Italy. E-mail: amenitsch@elettra.trieste.it

(*Received 4 August 1997; accepted 20 January 1998*)

The double-focusing high-flux wiggler beamline dedicated to small-angle X-ray scattering (SAXS) and wide-angle X-ray scattering (WAXS) at ELETTRA has gone into user operation recently. It has been designed specifically for time-resolved studies of non-crystalline and fibrous materials in the submillisecond time scale, and has been optimized for small-angle scattering measurements. An overview of the beamline status and of some representative results, highlighting the performance of the SAXS beamline, are given.

Keywords: small-angle X-ray scattering; time-resolved X-ray scattering; temperature jump; pressure jump.

1. Introduction

The new simultaneous small- and wide-angle X-ray scattering (SWAXS) station at ELETTRA, which is mainly dedicated to time-resolved studies (~1 ms), has proved to be a very practicable and promising new research tool for fast structure determination of non-crystalline and fibrous materials. In addition, the 57-pole ELETTRA wiggler source, combined with optics optimized for providing high flux and high brilliance, allows many other experiments to be performed, *e.g.* low-contrast solution scattering, grazing-incidence small-angle X-ray scattering (GISAXS), microspot scanning for determination of the texture of materials, like in SAXS tomography (Fratzl *et al.*, 1997), and X-ray peak profile analyses in the small- and wide-angle regime (Zehetbauer *et al.*, 1996).

The beamline is working at three fixed energies, namely 5.4, 8 and 16 keV; therefore the beamline is equally applicable to optically very thin (single muscle fibres) and optically thick (alloys or ceramics) specimens. The 8 keV monochromator chamber has been fully commissioned, since September 1996. The 5.4 and 16 keV monochromator chambers were installed in 1997, and their commissioning was recently completed.

After one year of user operation of the 8 keV branch, the beamline is still undergoing improvement, especially around the experimental stage, and this will give rise to new types and a new quality of experiments.

2. Source and optics

The source and the optics (see Fig. 1) have been described in detail elsewhere (Amenitsch *et al.*, 1995, 1997). Therefore, only a short description will be given here. A double-crystal monochromator containing three interchangeable pairs of asymmetric-cut Si(111) crystals with asymmetric-cut angles of 5.1, 12.3 and 19.5° for the three energies of 16, 8 and 5.4 keV, respectively, is used, on the one hand, as a beam splitter between the SAXS beamline and the diffraction beamline (the other branch line at the wiggler port); on the other hand, the monochromator shifts the beam 1.5 m in the vertical direction (Bernstorff *et al.*, 1998). Downstream, at a distance of 26.5 m from the source, a double-focusing toroidal mirror focuses the light with a demagnification factor of 2.77 onto the detector, which is situated 9.56 m after the mirror. The mirror consists of two identical Pt-coated Zerodur mirror segments (Carl Zeiss) with a total length of 1.5 m. The radii are 2.95 km and 6.53 cm for the longitudinal and sagittal curvatures, respectively.

The maximum spot size at the specimen is 5.4 × 1.8 mm (1.8 m upstream of the detector), but it can be reduced to 20 μm in diameter. The focal spot size measured with the detector is 1.5 × 0.6 mm (H × V), in good agreement with the calculated value of 1.3 × 0.6 mm.

For 8 keV photon energy and for the ring running with 250 mA at 2 GeV, the flux at the sample has been measured with a calibrated Si photodiode to be 2×10^{12} photons s^{-1} corresponding to a flux density of 4.5×10^{11} photons s^{-1} mm^{-2}.

At 8 keV and the maximum camera length of 2.8 m, the small-angle range between 1/1400 and 1/10 $Å^{-1}$ can be covered, and a wide-angle range between 1/9.4 and 1/1.2 $Å^{-1}$ is available. Fig. 2(*a*) shows data collected in 10 s from dry rat-tail tendon collagen, demonstrating that the initial goal of 1000 Å resolution has been reached. Fig. 2(*b*) is the diffraction pattern of *p*-Br-benzoic acid

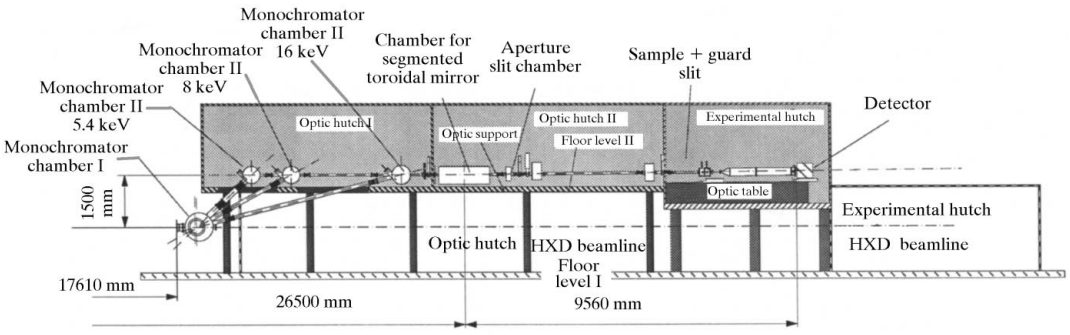

Figure 1
Schematic sketch of the beamline layout showing the double-crystal monochromator with its four chambers, the double-focusing mirror chamber and a simplified representation of the experimental hutch.

used for demonstrating the performance and calibration of the wide-angle regime.

3. Sample stage and detectors

The sample stage has been kept highly flexible and user-friendly. Together with the guard slit system it is mounted on an optical rail guide, which is adjustable from 0 to about 2800 mm from the detector. Furthermore, any other user equipment which does not fit the general dimensions of the sample stage can be mounted independently onto the optical bench, *e.g.* a magnet or stretching stages, within wide dimensional limits.

Several stages, such as temperature-jump (T-jump), pressure-jump (P-jump), stopped-flow *etc.* cells, are available for performing various experiments. The detector system consists of two linear Gabriel-type delay line detectors, one each for the small- and the wide-angle regions, and is based on a system described by Rapp *et al.* (1995). The readout system has been assembled with standard NIM components, whereas the histogramming memory and the time-frame generator are implemented on a PC card (HCI card, Hecus MBraun Graz X-ray Systems, Graz, Austria). The count-rate limit of the electronics is 1.6 MHz; however, maximum count rates around 100 kHz can be currently obtained due to space-charge effects in gas-filled single-wire detectors. A two-dimensional beamline detector is planned as standard equipment in the future; some user experiments have already been performed with user-provided two-dimensional CCD detectors.

4. Examples of performed experiments

Out of the wide variety of experiments performed on the beamline, just two examples have been selected to demonstrate the performance of the beamline.

As a standard unit, a T-jump device is available. It consists of an erbium-glass laser, emitting at a wavelength of 1.5 µm, which delivers 3–4 J within 2 ms onto the sample (Rapp & Goody, 1991). With this technique, phase transitions of lyotropic liquid crystals can be studied far from equilibrium. The sample (40 µl) is placed in a thermostated quartz glass capillary sample holder of diameter 1 mm and kept a few degrees below the transition temperature. The effect of rapid sample heating (about 10 K in 2 ms, *i.e.* 5000 K s^{-1}) is produced by IR absorption in water. As an example, the pretransition of dipalmitoyl-phosphatidylcholine (DPPC; 20% *w*/*w*) is given in Fig. 3. Directly after the laser shot, the generation of a thin liquid-crystalline phase L_{α^*} takes place, which coexists with the remaining small amounts of the original gel phase $L_{\beta'}$. In the first milliseconds after the heating pulse, the *d*-spacing of this intermediate with a value of 58 Å is clearly thinner than that of the usual liquid-crystalline phase L_α, but within a millisecond-to-second range its lamellar repeat increases until a *d*-spacing of about 67 Å is reached. In a second step the aliphatic chains relax to the all-*trans* conformation and the stable ripple phase $P_{\beta'}$ forms (Laggner *et al.*, 1991; Rappolt, 1995).

Another standard technique used at this beamline are P-jump experiments (Steinhart *et al.*, 1998), in which the pressure of the sample is changed within 5–10 ms from 1 up to 3000 bar or *vice versa*. In Fig. 4 the P-jump of dioleoyl-phosphatidylethanolamine (DOPE) in excess water from 150 to 2290 bar at 293 K is presented. The diffraction pattern of the transitions is sampled in 5 ms frames showing the instantaneous transition from the inverted hexagonal phase H_{II} into the lamellar liquid-crystalline phase L_α and the slow change into the lamellar gel phase L_β with a lag time of about 4 s.

5. Conclusions

The main objective of building the SWAXS beamline at ELETTRA was to provide new opportunities for fast time-resolved studies on molecular rearrangements of nanomaterials of biological and/or technological significance. Providing optimal

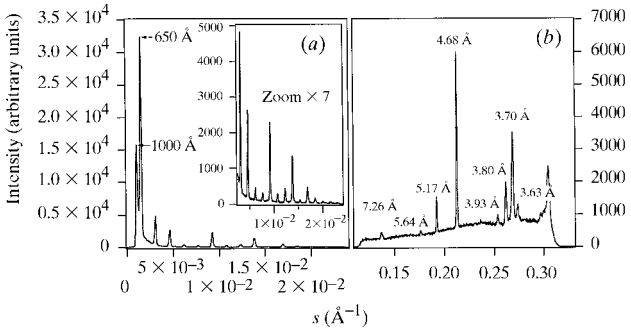

Figure 2
(*a*) Raw data of the diffraction pattern of dry rat-tail tendon with a *d*-spacing of 650 Å taken at a detector-to-sample distance of 2.3 m. The exposure time was 10 s. (*b*) Raw data of *p*-Br-benzoic acid demonstrating the WAXS performance in the range 1/9.4–1/3.2 Å.

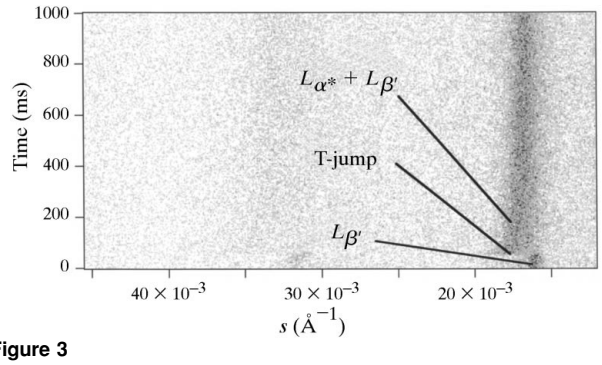

Figure 3
Contour plot of the pretransition of dipalmitoyl-phosphatidylcholine (DPPC, 20% *w*/*w*) in the SAXS regime, which has been induced by a rapid T-jump (>40 K within 2 ms) from about 299 K. The phase transition $L_{\beta'}$–L_{α^*} is visible.

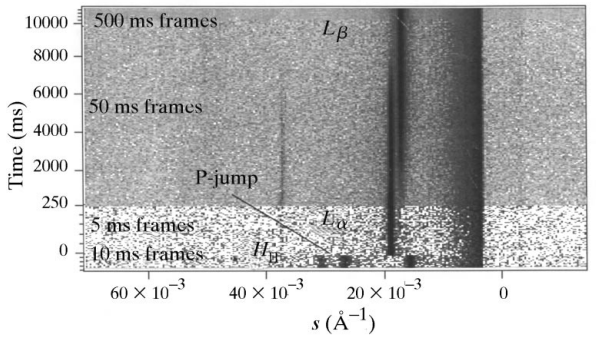

Figure 4
P-jump experiment on dioleoyl-phosphatidylethanolamine in excess water at T = 293 K, jumping from 150 to 2290 bar. The sample is undergoing the phase transitions H_{II}–L_α–L_β.

photon flux density (with $\sim 5 \times 10^{11}$ photons s^{-1} mm^{-2} being among the best of systems presently existing) is but one task in this pursuit. Equally important are two other aspects, which are generally less well taken care of: time resolution and efficiency of the detector, and jump-relaxation technologies required to induce fast non-equilibrium.

The efforts in providing a set of first-class tools for fast sample triggering, T-jump, P-jump or stopped-flow mixing have been tested exhaustively in the first user period of the beamline, and have proven excellently suited for many purposes in biophysical and materials science experiments.

However, the bottleneck still to be overcome lies in the speed of detection. (With present technologies the overall counting rates are of the order of 1 MHz.) Serious efforts are necessary to overcome this situation, because only when this is accomplished, will the full potential of synchrotron radiation optics for microstructure research become usable.

The authors are very grateful to the staff members of the Austrian Academy of Sciences (IBR, Graz, Austria) and of the Sincrotrone Trieste who have contributed to the beamline project. We especially thank M. Steinhart, R. Menk, C. Krenn and G. Papst for their help in the assembly and in the running of the station.

References

Amenitsch, H., Bernstorff, S., Kriechbaum, M., Lombardo, D., Mio, H., Rappolt, M. & Laggner, P. (1997). *J. Appl. Cryst.* **30**, 872–876.
Amenitsch, H., Bernstorff, S. & Laggner, P. (1995). *Rev. Sci. Instrum.* **66**, 1624–1626.
Bernstorff, S., Amenitsch, H. & Laggner, P. (1998). *J. Synchrotron Rad.* In the press.
Fratzl, P., Jakob, H., Rinnerthaler, S., Roschger, P. & Klaushofer, K. (1997). *J. Appl. Cryst.* **30**, 765–769.
Laggner, P., Kriechbaum, M. & Rapp, G. (1991). *J. Appl. Cryst.* **24**, 836–842.
Rapp, G., Gabriel, A., Dosière, M. & Koch, M. H. J. (1995). *Nucl. Instrum. Methods Phys. Res. A*, **375**, 178–182.
Rapp, G. & Goody, R. S. (1991). *J. Appl. Cryst.* **24**, 857–865.
Rappolt, M. (1995). Doctoral thesis, University of Hamburg, Germany.
Steinhart, M., Kriechbaum, M., Pressl, K., Amenitsch, H., Laggner, P. & Bernstorff, S. (1998). *Rev. Sci. Instrum.* Submitted.
Zehetbauer, M., Kral, R., Ungar, T., Borbely, A., Ortner, B., Bernstorff, S. & Amenitsch, H. (1996). *ELETTRA News 8,* http://www.elettra.trieste.it/.